

STARK EFFECT IN SOME NANOSTRUCTURES

Adelina Miteva

Space and Solar-Terrestrial Research Institute – Bulgarian Academy of Sciences
e-mail: admiteva@phys.bas.bg

Key words: square-shaped (rectangular) semiconductor quantum wells, electric field effect, tight-binding method, AlGaAs, quantum confined Stark effect, nanostructures

Abstract: The motivation of this research is the tremendous interest in semiconductor nanostructures. The aim of this paper is to conduct realistic numerical tight-binding calculations for the electron states of some semiconductor nanostructures, namely in square-shaped AlGaAs quantum wells with different depths and in the presence of a constant electric field. The paper shows some of these results.

ЩАРК ЕФЕКТ В НЯКОИ НАНОСТРУКТУРИ

Аделина Митева

Институт за космически и слънчево-земни изследвания – Българска академия на науките
e-mail: admiteva@phys.bas.bg

Резюме: Работата е мотивирана от небивалия в наши дни интерес към нанотехнологиите и полупроводниковите наноструктури. Целта на това изследване е провеждането на реалистични числени пресмятания по метода на силната връзка на електронните състояния в някои наноструктури. Тук са пресметнати правоъгълни квантови ями от AlGaAs с различни дълбочини и в присъствието на постоянно електрично поле. Представени са някои от получените резултати.

1. Introduction

Nowadays, semiconductor nanostructures find practical applications in all important fields of industry and in our daily life. A very important area for such applications is their actual and potential applications in various electro-optical devices. Modern electronic and optoelectronic devices are approaching nanometric dimensions and employ semiconductor nanostructures. Many semiconductor devices with built-in quantum wells work under application of an electric field. Investigation of the electric-field dependence of electronic and optical properties in semiconductor nanostructures (quantum wells) is of great interest, due to the possibility of making various optoelectronic devices, and thus optimize nanostructure-based devices. Atomistic approaches become necessary for modeling structural, electronic and optical properties of such nanostructures and nanostructured devices [1-3].

The aim of the present work is to conduct realistic numerical calculations with one of the methods, which is widely used for atomistic investigation of semiconductor nanostructures – the semiempirical tight binding (TB) method. Numerical calculations within the framework of a realistic tight-binding model for the electron bound states of some semiconductor nanostructures, namely of square-shaped (rectangular) quantum wells (SQWs) with different depths, in the presence of a constant electric field have been made.

We study SQWs with thickness of 44 MLs. One ML (monolayer) equals two atomic layers and 1ML equals 2.825×10^{-10} m. The SQWs are formed in the system of $\text{Al}_x\text{Ga}_{1-x}\text{As}$ / $\text{Al}_x\text{Ga}_{1-x}\text{As}$ / $\text{Al}_x\text{Ga}_{1-x}\text{As}$. The Al concentration x in the barriers $\text{Al}_x\text{Ga}_{1-x}\text{As}$ is $x = 0.36$ for all SQWs under study. The Al concentration x in the well regions $\text{Al}_x\text{Ga}_{1-x}\text{As}$ is different and takes four values: $x = 0$, $x = 0.03$; $x = 0.06$; $x = 0.12$, respectively for the four SQWs under study (see Fig. 1). We can see in Fig. 1 that the concentration profile of Al in SQWs makes one SQW deeper than the other. The deepest SQW has a concentration of Al in the quantum well (QW) region $x = 0$. And the most shallow SQW has a concentration of Al in the quantum well (QW) region $x = 0.12$.

We calculate the electron bound states, the hole bound states and their spatial distributions without and with applying a various values of the constant longitudinal electric field F . The electric field is applied parallel to the growth axis [001]. We calculate also the energies of the optical transitions $E(C1-HH1)$, $E(C1-LH1)$, $E(C2-HH2)$ and their Stark shifts. The Stark shift is a reduction of the optical transition energy in a QW under application of an electric field.

Similar results concerning the calculation of the ground state energies of the conduction $E(C1)$, $E(C2)$ and valence $E(HH1)$, $E(LH1)$, $E(HH2)$ bound states in three QWs in dependence of applied constant electric field F were already published and discussed in [4].

2. Model and method

We study $Al_xGa_{1-x}As / Al_{1-x}Ga_xAs / Al_xGa_{1-x}As$ SQWs (001) with the square-shaped (or rectangular) well structures (Fig. 1). The electric field is applied parallel to the growth axis [001]. Similar structures are partially investigated theoretically in [4,5]. We use the sp^3s^* spin-dependent semi-empirical tight-binding model as it is described in [6]. The virtual crystal approximation is used for the description of the TB parameters $TB(x)$ of the alloy $Al_xGa_{1-x}As$:

$$TB(x) = x \cdot TB(AlAs) + (1-x) \cdot TB(GaAs).$$

We use surface Green function matching technique, developed and applied in [7] in order to calculate the Green function of the infinite system containing the finite inhomogeneous slab. We define the presence of an external static electric field (see [8,9]) by adding an linearly varying with the distance term Δ_n to the diagonal elements of the TB Hamiltonian matrix:

$$(1) \quad TB(n,x) = TB(x) + \Delta_n, \quad \text{and}$$

$$(2) \quad \Delta_n = (n-1) \cdot F \cdot (a/4),$$

where a is the lattice constant, F is the intensity of the longitudinal constant electric field, $TB(x)$ are the diagonal TB parameters without an electric field for the bulk material with Al concentration x , and n is the number of the layer (i.e. layer index) in QW. The electric field is applied to the structure under study at two points in the well regions ($Al_xGa_{1-x}As$) at the two edges of the SQWs. The width of the four SQWs is 44 MLs (which is approximately 125 Å; or 12.43 nm). The zero value of the intensity of applied electric field F is defined at the point which corresponds to the first ML from the left edge of the QWs. In our numerical calculations we use a range of electric fields, from -212.4 to $+212.4$ kV/cm with 70.8 kV/cm step. We also made calculations for the conventional square-shaped QW (SQW) (with Al composition x equals 0) in order to compare it with our results. The SQWs have a 44 MLs (125 Å) $Al_xGa_{1-x}As$ wells and $Al_{0.36}Ga_{1-0.36}As$ barriers. All calculations are made at the center of the two-dimensional Brillouin zone.

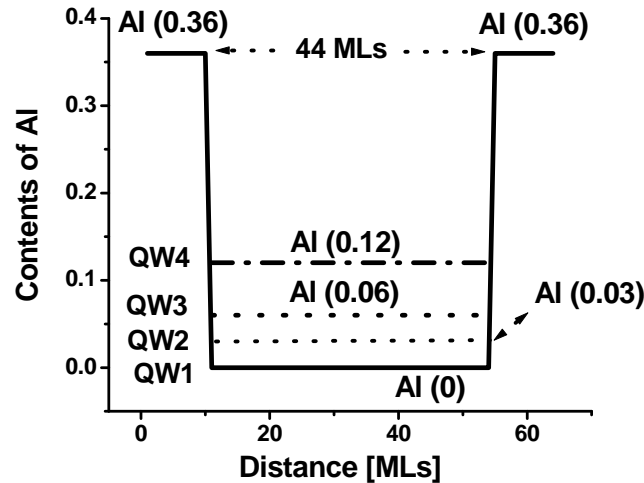


Fig. 1. Schematic band diagram of four SQWs without application of a constant electric field. SQW number 1 (indicated as QW1 on the figure) consists of pure GaAs. SQW2 has Al concentration $x = 0.03$. SQW3 has Al concentration $x = 0.06$. SQW4 has Al concentration $x = 0.12$. In four cases we have at the barriers the Al concentration of the alloy composition $x = 0.36$.

3. Results and discussion

The influence of the applied electric field F on the concentration profile of the SQW follows: the electric field makes the concentration profile inclined. The direction of the slope of this profile depends on the sign and the value of the applied electric field F . Calculated main bound electron and hole

energies of the four SQWs under study without and in the presence of a constant electric field were already discussed in [4]. EC1 and EC2 are the conduction band bound states, and EHH1, ELH1 and EHH2 are the valence band bound states. For all four SQWs the behavior of these energies is similar: they decrease or increase with increasing or decreasing the applied electric field.

And for all RQWs the transition energies decrease with increasing applied electric field [4]. Consequently we can say that the increasing the concentration of Al in RQWs gives larger and better Stark shifts of the transition energies.

We see in Fig. 2 the RQW of type $\text{Al}_{0.36}\text{Ga}_{1-0.36}\text{As} / \text{Al}_{0.06}\text{Ga}_{1-0.06}\text{As} / \text{Al}_{0.36}\text{Ga}_{1-0.36}\text{As}$ which corresponds to RQW 3 from Fig. 1. Here, in Fig. 2, we see the influence of the electric field on the concentration profile of the RQW. The electric field makes the concentration profile inclined. The direction of the slope of this profile depends on the sign and the value of the applied electric field F .

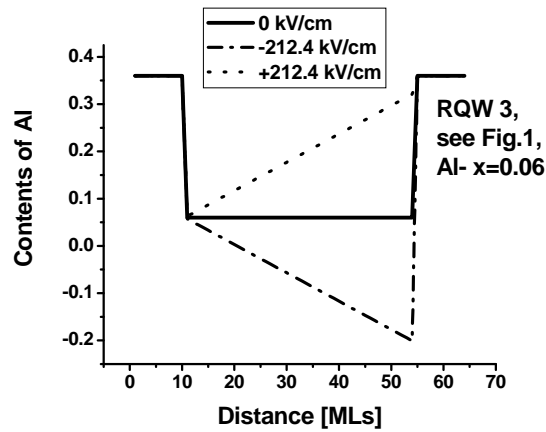


Fig. 2. Schematic band diagram of the concentration profile of RQW3 (see Fig. 1) without and with the application of a constant electric field F of the value 212.4 kV/cm. RQW number 3 (RQW 3) has Al concentration $x = 0.06$. The Al concentration of the alloy composition is $y = 0.36$ at the barriers.

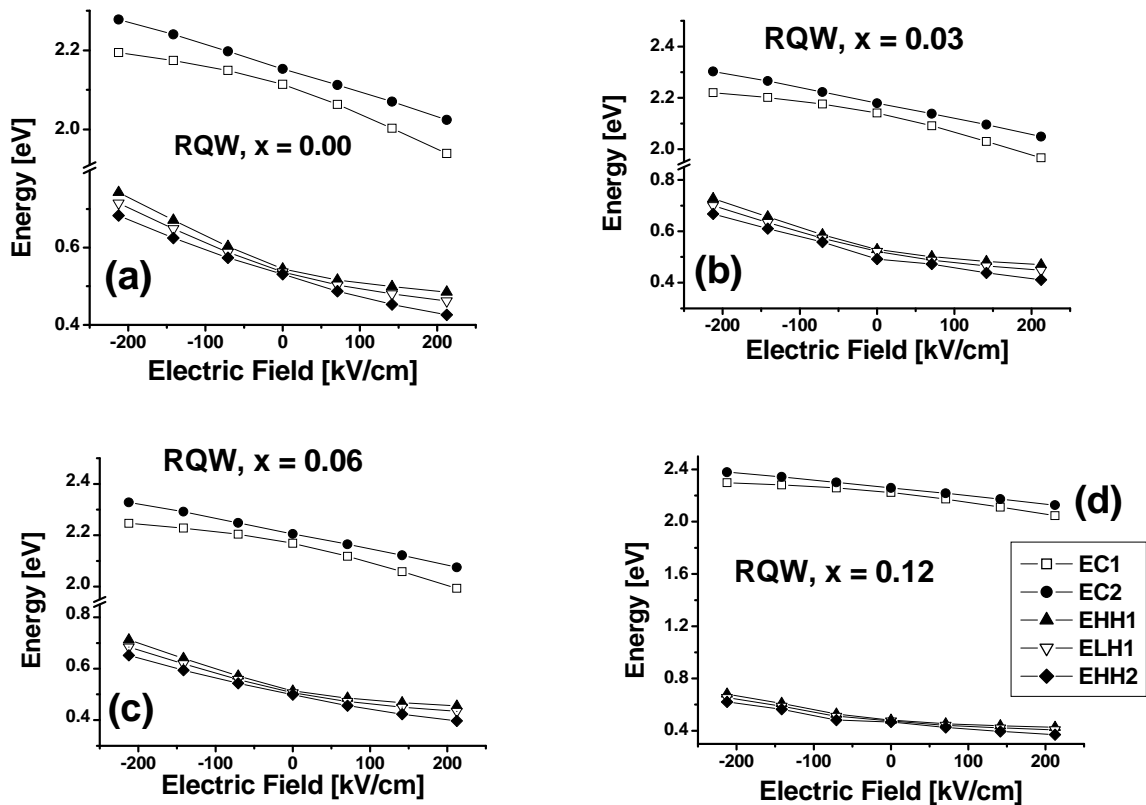


Fig. 3. Main calculated bound electron and hole energies of the four RQWs without and with the application of a constant electric field F . Al concentration x for each RQW is indicated on the figure.

Fig. 3 shows the calculated main bound electron and hole energies of the four RQWs under study without and in the presence of a constant electric field. EC1 and EC2 are the conduction band bound states, and EHH1, ELH1 and EHH2 are the valence band bound states. They are indicated on the Fig. 3. And also as it is indicated on the figure: Fig. 3 (a) – RQW with Al contents $x = 0.0$; Fig. 3 (b) – RQW with Al contents $x = 0.03$; Fig. 3 (a) – RQW with Al contents $x = 0.06$; Fig. 3 (a) – RQW with Al contents $x = 0.12$. For all four RQWs the behavior of the energies is similar: they decrease or increase with increasing or decreasing the applied electric field.

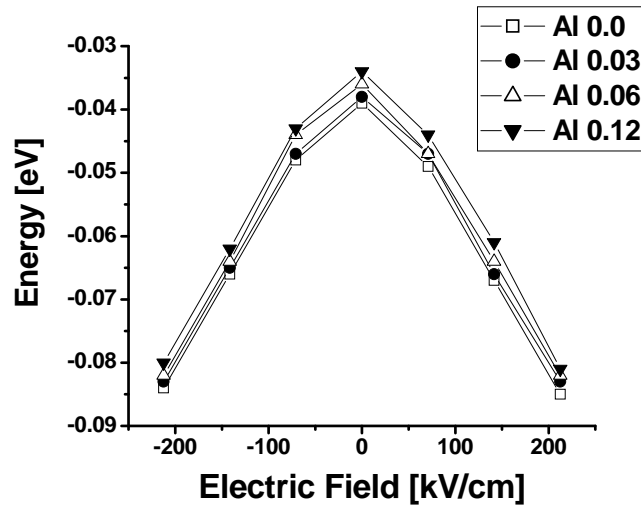


Fig. 4. Transition energies $E(C1-C2)$ as a function of applied electric field for the RQWs under study. RQWs are indicated on the figure with the contents of Al.

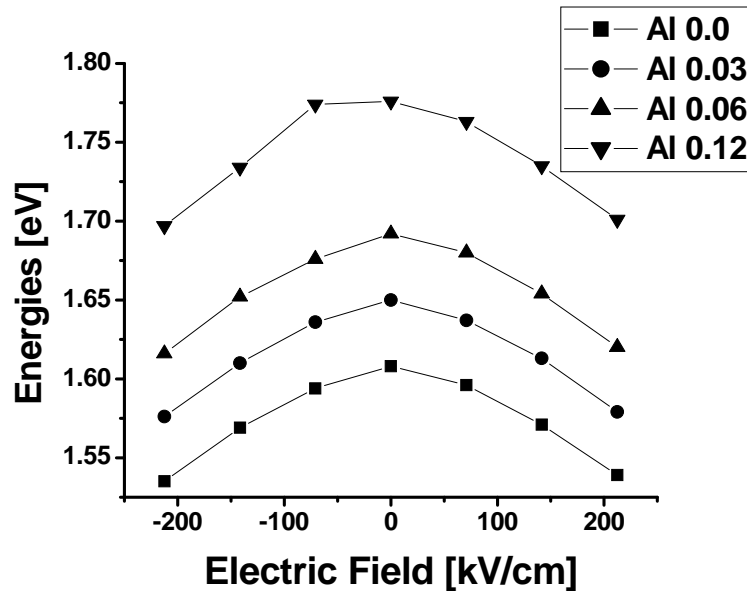


Fig. 5. Transition energies $E(C2-HH1)$ as a function of applied electric field for the RQWs under study. RQWs are indicated on the figure with the contents of Al.

Fig. 4 shows the transition energies $E(C1-C2)$. As we can see they are larger for RQW with the largest contents of Al. With increasing the concentration of Al in RQWs the transition energy $E(C1-C2)$ increases. And for all RQWs the transition energies decrease with increasing applied electric field. Consequently we can say that the increasing the concentration of Al in RQWs gives larger and better Stark shifts.

Fig. 5 shows the transition energies $E(C2-HH1)$. As we can see they are larger for RQW with the largest contents of Al. With increasing the concentration of Al in RQWs the transition energy $E(C2-HH1)$ increases. And for all RQWs the transition energies decrease with increasing applied electric field. Consequently we can say the same as for the transition energies $E(C1-C2)$ (see Fig. 4), namely that the increasing the concentration of Al in RQWs gives larger and better Stark shifts under application of the same values of electric field.

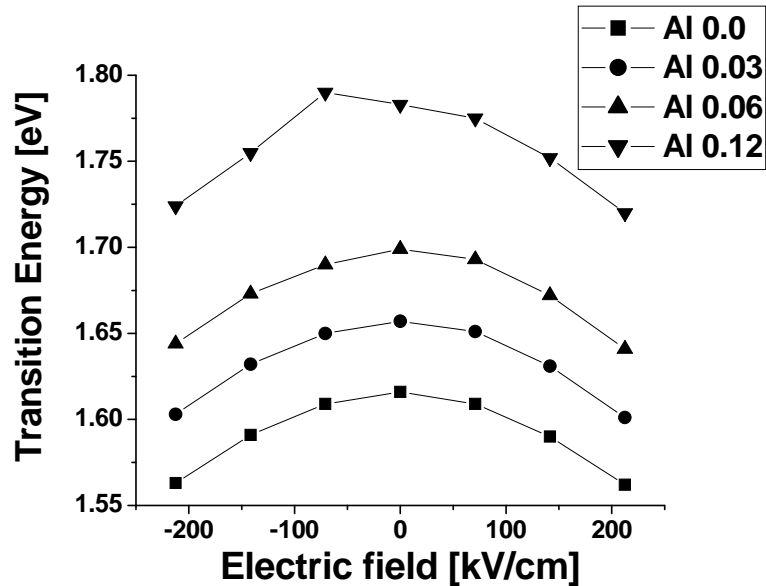


Fig. 6. Transition energies $E(C2-LH1)$ as a function of applied electric field for the RQWs under study. RQWs are indicated on the figure with the contents of Al.

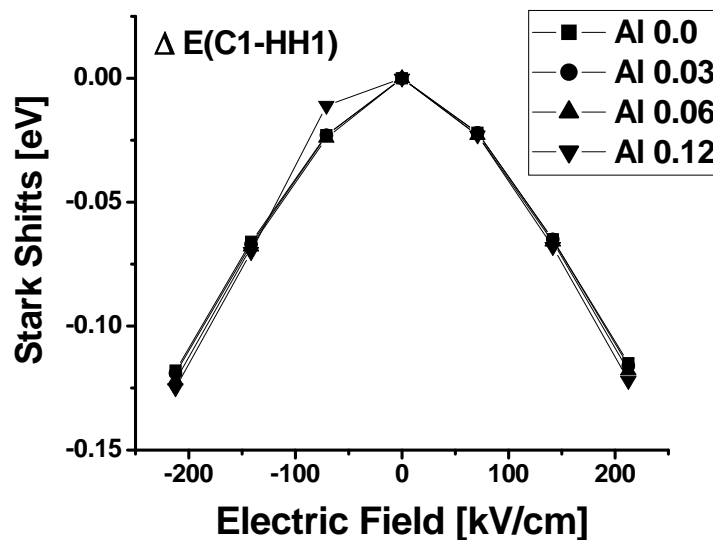


Fig. 7. Stark shifts of the main transition energies $E(C1-HH1)$ as a function of applied electric field for all of the SQWs under study. SQWs are indicated on the figure with the contents of Al.

Fig. 6 shows the transition energies $E(C2-LH1)$. As we can see they are larger for RQW with the largest contents of Al. With increasing the concentration of Al in RQWs the transition energy $E(C2-LH1)$ increases. And for all RQWs the transition energies decrease with increasing applied electric

field. Consequently we can say the same as for the transition energies $E(C1-C2)$ and for $E(C2-HH1)$ (see Fig. 4 and see Fig. 5), namely that the increasing the concentration of Al in RQWs gives larger and better Stark shifts under application of the same values of electric field.

Fig. 7. shows the Stark shifts of the main transition energies $E(C1-HH1)$. As we can see they are larger for SQW with the largest contents of Al. With increasing the concentration of Al in SQWs the Stark shifts of the transition energy $E(C1-HH1)$ increases. And for all SQWs the transition energy Stark shifts decrease with decreasing applied electric field. Consequently we can say the same as for the transition energies $E(C1-C2)$ (see Fig. 4 in [4]), namely that the increasing the concentration of Al in RQWs gives larger and better Stark shifts under application of the same values of electric field.

4. Conclusion and future work

We conduct realistic numerical TB calculations of the electron bound states, the hole bound states and their spatial distributions without and with applying a various values of the constant longitudinal electric field F for four types of SQWs with different depth. We can say that the results from the TB calculations, such in this work, help to study the physics of the nanostructures in the presence of applied electric field intensities. Such investigations that make possible to study in details the Stark shifts of the electronic and hole states and their spatial distributions, the subband spectra and intersubband transitions of electrons, are very promising in looking for quantum well structures that provides good Stark effect characteristics for potential device applications. Such investigation will help us to find a QW potential profile with better Stark effect characteristics. The investigation of the electric field effects on the optical properties of the QW structures with graded gap potential profiles (not conventional SQWs) is essential for the optimization of QW-based devices. The work is in progress in this direction.

References:

1. A l f e r o v, Z. I., Rev. Mod. Phys., vol. 73, 2001, pp. 769-782.
2. B a s t a r d, G., Wave mechanics applied to semiconductor heterostructures, 1988, (Les Ulis Cedex: Les Edition de Physique)
3. D i C a r l o, A., Semicond. Sci. Technol. vol. 18, 2003, pp. R1-R31.
4. M i t e v a, A., <http://mtf65.tu-sofia.bg>, 26-та МЕЖДУНАРОДНА НАУЧНА КОНФЕРЕНЦИЯ 65 ГОДИНИ МАШИННО-ТЕХНОЛОГИЧЕН ФАКУЛТЕТ, 13 – 16. СЕПТЕМВРИ, 2010, Созопол, БЪЛГАРИЯ, Технически университет, гр.София, ISBN: 978-954-438-854-6, pp. 283-288.
5. V l a e v, S. J., A. M. M i t e v a, D. A. C o n t r e r a s - S o l o r i o and V. R. V e l a s c o, Surf. Sci., vol. 424, 1999, pp. 331-339.
6. V l a e v, S. J., V. R. V e l a s c o and F. G a r c i a - M o l l n e r, Phys. Rev. B, vol. 49, 1994, pp. 11222-1229.
7. G a r c i a - M o l l n e r, F. and V. R. V e l a s c o, Theory of Single and Multiple Interfaces. The Method of Surface Green Function Matching (World Scientific, Singapore, 1993).
8. V l a e v, S. J., A. M. M i t e v a, D. A. C o n t r e r a s - S o l o r i o and V. R. V e l a s c o, Superlattces Microstruct., vol. 26, 1999, pp. 325-332.
9. M i t e v a, A. M., S. J. V l a e v, V. T. D o n c h e v and L. M. G a g g e r o - S a g e r, Rev. Mex. Fis. S, vol. 53, 2007, pp. 74-77.